Highly simplified device for measuring the intensity and phase of picosecond pulses

Jacob Cohen,[1,*] Dongjoo Lee,[2] Vikrant Chauhan,[1] Peter Vaughan,[1]
and Rick Trebino[1]

[1]*Department of Physics, Georgia Institute of Technology, 837 State St., Atlanta 30332, Georgia, USA*
[2]*Swamp Optics, 6300 Powers Ferry Road, Suite 600-345, Atlanta 30339-2919, Georgia, USA*
*jcohen7@gatech.edu

Abstract: We demonstrate an extremely simple frequency-resolved-optical-gating (GRENOUILLE) device for measuring the intensity and phase of relatively long—ps—pulses. In order to achieve the required high spectral resolution and large temporal range, it uses a few-cm-thick second-harmonic-generation crystal in the shape of a pentagon. This has the additional advantage of reducing the device's total number of components to as few as three simple easily aligned optics, making it the simplest device ever developed for complete pulse measurement. We report complete intensity-and-phase measurements of pulses up to 15ps long with a time-bandwidth product of 21.

©2010 Optical Society of America

OCIS codes: (320.0320) Ultrafast optics; (320.7100) Ultrafast measurements.

References and links

1. A. M. Weiner, "Femtosecond pulse shaping using spatial light modulators," Rev. Sci. Instrum. **71**(5), 1929–1960 (2000).
2. C. Dorrer, "High-speed measurements for optical telecommunication systems," IEEE J. Sel. Top. Quantum Electron. **12**(4), 843–858 (2006).
3. P. O'Shea, M. Kimmel, X. Gu, and R. Trebino, "Highly simplified device for ultrashort-pulse measurement," Opt. Lett. **26**(12), 932–934 (2001).
4. R. Trebino, *Frequency-Resolved Optical Gating: The Measurement of Ultrashort Laser Pulses* (Kluwer Academic Publishers, 2002).
5. C. Iaconis, and I. A. Walmsley, "Spectral phase interferometry for direct electric-field reconstruction of ultrashort optical pulses," Opt. Lett. **23**(10), 792–794 (1998).
6. C. Dorrer, B. de Beauvoir, C. Le Blanc, S. Ranc, J. P. Rousseau, P. Rousseau, J. P. Chambaret, and F. Salin, "Single-shot real-time characterization of chirped-pulse amplification systems by spectral phase interferometry for direct electric-field reconstruction," Opt. Lett. **24**(22), 1644–1646 (1999).
7. C. Dorrer, N. Belabas, J.-P. Likforman, and M. Joffre, "Spectral resolution and sampling issues in Fourier-transform spectral interferometry," J. Opt. Soc. Am. B **17**(10), 1795–1802 (2000).
8. J. R. Birge, R. Ell, and F. X. Kärtner, "Two-dimensional spectral shearing interferometry for few-cycle pulse characterization," Opt. Lett. **31**(13), 2063–2065 (2006).
9. M. A. Foster, R. Salem, D. F. Geraghty, A. C. Turner-Foster, M. Lipson, and A. L. Gaeta, "Silicon-chip-based ultrafast optical oscilloscope," Nature **456**(7218), 81–84 (2008).
10. D. H. Broaddus, M. A. Foster, O. Kuzucu, A. C. Turner-Foster, K. W. Koch, M. Lipson, and A. L. Gaeta, "Temporal-imaging system with simple external-clock triggering," Opt. Express **18**(13), 14262–14269 (2010).
11. C. Froehly, A. Lacourt, and J. C. Vienot, "Time impulse response and time frequency response of optical pupils: experimental confirmations and applications," Nouv. Rev. Opt. **4**(4), 183–196 (1973).
12. L. Lepetit, G. Cheriaux, and M. Joffre, "Linear techniques of phase measurement by femtosecond spectral interferometry for applications in spectroscopy," J. Opt. Soc. Am. B **12**(12), 2467–2474 (1995).
13. P. Bowlan, P. Gabolde, A. Shreenath, K. McGresham, R. Trebino, and S. Akturk, "Crossed-beam spectral interferometry: a simple, high-spectral-resolution method for completely characterizing complex ultrashort pulses in real time," Opt. Express **14**(24), 11892–11900 (2006).
14. J. Cohen, P. Bowlan, V. Chauhan, and R. Trebino, "Measuring temporally complex ultrashort pulses using multiple-delay crossed-beam spectral interferometry," Opt. Express **18**(7), 6583–6597 (2010).
15. C. Dorrer, and I. Kang, "Linear self-referencing techniques for short-optical-pulse characterization [Invited]," J. Opt. Soc. Am. B **25**(6), A1–A12 (2008).

16. X. Gu, L. Xu, M. Kimmel, E. Zeek, P. O'Shea, A. P. Shreenath, R. Trebino, and R. S. Windeler, "Frequency-resolved optical gating and single-shot spectral measurements reveal fine structure in microstructure-fiber continuum," Opt. Lett. **27**(13), 1174–1176 (2002).
17. H. Fuchs, D. Woll, T. Ulm, and J. A. L'Huillier, "High resolution FROG system for the characterization of ps laser pulses," Appl. Phys. B **88**(3), 393–396 (2007).
18. C. Radzewicz, P. Wasylczyk, and J. S. Krasinski, "A poor man's FROG," Opt. Commun. **186**(4-6), 329–333 (2000).
19. S. Akturk, M. Kimmel, P. O'Shea, and R. Trebino, "Extremely simple device for measuring 20-fs pulses," Opt. Lett. **29**(9), 1025–1027 (2004).
20. S. Akturk, M. Kimmel, and R. Trebino, "Extremely simple device for measuring 1.5-microm ultrashort laser pulses," Opt. Express **12**(19), 4483–4489 (2004).
21. S. Akturk, M. Kimmel, P. O'Shea, and R. Trebino, "Measuring pulse-front tilt in ultrashort pulses using GRENOUILLE," Opt. Express **11**(5), 491–501 (2003).
22. D. Lee, and R. Trebino, "Extremely simple device for measuring ultrashort pulses in the visible," in *Lasers and Electro-Optics, 2009 and 2009 Conference on Quantum electronics and Laser Science Conference. CLEO/QELS 2009. Conference on*, 2009), 1–2.
23. D. Lee, Z. Wang, X. Gu, and R. Trebino, "Effect—and removal—of an ultrashort pulse's spatial profile on the single-shot measurement of its temporal profile," J. Opt. Soc. Am. B **25**(6), A93 (2008).
24. P. O'Shea, S. Akturk, M. Kimmel, and R. Trebino, "Practical issues in ultra-short-pulse measurements with 'GRENOUILLE'," Appl. Phys. B **79**(6), 683–691 (2004).
25. D. Lee, Z. Wang, X. Gu, and R. Trebino, "Effect—and removal—of an ultrashort pulse's spatial profile on the single-shot measurement of its temporal profile," J. Opt. Soc. Am. B **25**(6), A93–A100 (2008).
26. V. G. Dmitriev, G. G. Gurzadyan, and D. N. Nikogosyan, *Handbook of nonlinear optical crystals,* 3rd ed. (Springer-Verlag, Berlin, Germany, 1991).
27. X. Liu, R. Trebino, and A. V. Smith, "Numerical Simulations of the Ultrasimple Ultrashort-Laser-Pulse Measurement Technique, GRENOUILLE," in OSA Technical Digest Series (CD) (Optical Society of America, 2007), JThD8.
28. P. A. Jansson, and M. Richardson, "Deconvolution of Images and Spectra, 2nd Edition," Opt. Eng. **36**(11), 3224–3225 (1997).

1. Introduction

Ultrashort laser pulses in the few-ps range are important for many applications, from telecommunications to pulse shaping [1,2]. As a result, their measurement is also important. Interestingly, however, while measuring fs pulses has become almost routine [3,4], measuring longer, ps, pulses can be challenging due to the need for a relatively large temporal range and relatively high spectral resolution.

There are a number of methods for measuring ultrashort pulses in general, of which frequency resolved optical gating (FROG) [4] and spectral phase interferometry for direct electric field reconstruction (SPIDER) [5] are the most popular. However, the longest pulses that SPIDER has been able to measure have been ~500fs in length [6], and it is difficult to extend SPIDER to longer pulses because its required internally generated double pulse reduces its spectral resolution by about a factor of 5 [7]. Although a spatially encoded arrangement for SPIDER overcomes this spectral-resolution issue, both versions still suffer from difficult calibration issues [8], which are less problematic for longer pulses but remain severe.

Several time-domain techniques based on temporal imaging can measure at least the temporal intensity of ps pulses [9,10] by stretching them to ns in length. Streak cameras can also measure the temporal intensity of ps pulses. Additionally, several temporal- and spectral-interferometry techniques have also been used to measure few-ps pulses [11–14]. In addition, a number of linear self-referencing techniques use temporal modulators to measure pulses up to 100ps long with high sensitivity [15]. However, all these techniques require precise electrical synchronization of the pulse under test with the temporal modulator or require a well-characterized reference pulse.

FROG has been more successful in addressing the ps regime. Cross-correlation FROG (XFROG), which uses a well-characterized reference pulse, has measured an extremely complex, several-ps pulse with a time-bandwidth product (TBP) of several thousand [16]. Using a large high-resolution spectrometer, Fuchs, *et al.* [17], have engineered a FROG (which is self-referenced) capable of measuring pulses up to 80ps long. And FROGs are

commercially available for measuring few-ps pulses. Nevertheless, even a technique that works well is worth simplifying.

In this publication, we introduce an extremely simple FROG capable of measuring pulses up to 15ps in length. As a FROG technique, it is complete, yielding the intensity and phase vs. time and frequency with only easily removed, trivial ambiguities. It is passive and so doesn't require synchronization or a reference pulse. It is a variation of the very simple GRENOUILLE technique currently in common use [3]. GRENOUILLE has the advantages that, in its standard form, it comprises as few as only four simple optics, has no beam splitters or beam recombining optics and so is extremely easy to align, and does not require the use of extremely thin second-harmonic-generation (SHG) crystals, which can be difficult to manufacture and which limit device sensitivity. Indeed, GRENOUILLE actually *requires* a thick crystal because, unlike traditional pulse-measurement devices, it uses the crystal phase-matching bandwidth for its spectral resolution [18], and the thicker the crystal the better the spectral resolution. The thick crystal also improves the device sensitivity. Indeed, the ps version of GRENOUILLE that we introduce here involves a several-cm crystal and so is particularly high-spectral resolution. Like previous GRENOUILLEs, it is also easily aligned and, in fact, is composed of as few as only *three* simple optics, to our knowledge the simplest pulse-measurement technique ever developed.

In previous work, GRENOUILLE has measured Ti:Sapphire (700-1000nm) pulses from 20fs to ~1ps in length [19] and telecommunications pulses at 1.5μm [20] over a similar pulse-length range. In addition, we have shown that GRENOUILLE also naturally measures pulse-front tilt and spatial chirp without any modifications [21]. Most recently, we have extended GRENOUILLE's spectral range to include pulses in the visible (460-740nm) [22], and we have found that it is much more resilient to beam-shape-induced distortions than traditional single-shot autocorrelators and FROGs [23].

GRENOUILLE has not yet, however, measured pulses longer than ~2ps. This is because the simultaneous need for both a large delay range and high spectral resolution is challenging. Here we solve these problems and extend GRENOUILLE to pulses as long as ~15ps. Our solution is the use of a unique, thick *pentagonal* SHG crystal. Also, we show that this GRENOUILLE can measure even complex pulses and here measure a pulse with a time-bandwidth product of 21. Finally, we consider GRENOUILLE's current limits with regard to long-pulse measurement.

2. GRENOUILLE and its extension to longer pulses

A pulse with a temporal length of Δt can exhibit spectral features as narrow as $\delta\omega$ ~$2\pi/\Delta t$ wide, which must be resolved for an accurate measurement. Specifically, a 10ps pulse at 800nm has spectral features of ~0.1nm, so the required spectral resolution is ~0.05nm. In a GRENOUILLE, the spectral resolution is the crystal's phase-matching bandwidth, which is inversely proportional to the crystal thickness, so a thick and/or a dispersive crystal is required. Additionally, a large delay range is required, which, for 10ps pulses, is ~20ps, or ~4mm separation in the crystal between the two pulse replicas, which is a large distance when simply crossing beams at an angle as is done in GRENOUILLE and other pulse-measurement devices in order to achieve the required delay range.

To achieve these goals, we make two device modifications. First, we use a several-cm-thick highly dispersive crystal ($LiIO_3$) to provide the required improved spectral resolution (see Fig. 1). Secondly, we use a very large beam crossing angle–more than twice as large as previous versions. This latter condition sounds easy, but in fact proved the most challenging task in designing this device. GRENOUILLE's convenience stems from its use of a Fresnel biprism to split the pulse into two and cross the resulting replicas without the need for any alignment (see Fig. 2). And it proved impossible to use it to achieve a large beam crossing angle.
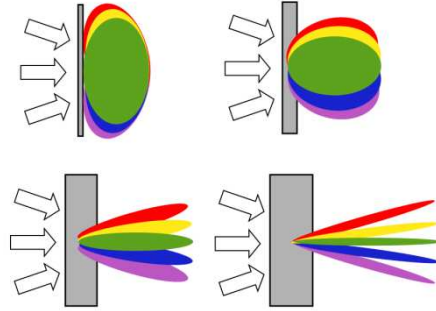
Fig. 1. Polar plots of SHG efficiency vs. output angle for various colors of a broadband beam impinging on a SHG crystal. Note that, for a thin crystal (upper left), the SHG efficiency varies slowly with angle for all colors, leading to a large phase-matching bandwidth for a given angle. As the crystal thickness increases, the polar plots become narrower, leading to very small phase-matching bandwidths. The thinnest crystal shown here would be required for all pulse-measurement techniques. GRENOUILLE, however, uses a thick crystal (lower right) to spectrally resolve the autocorrelation signal, yielding a FROG trace — without the need for a spectrometer.
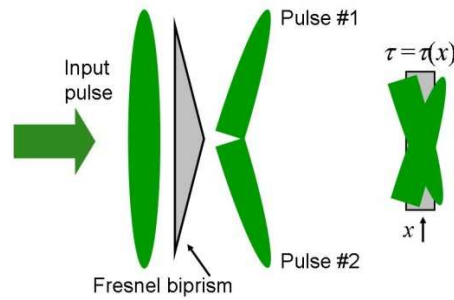

Fig. 2. Single-shot FROG measurements involve crossing large beams at a large angle, so that the relative delay between the two beams varies transversely across the crystal (right). The delay varies along x, the dimension in which the two beams are crossing. This can be accomplished more easily and without the need for alignment using a prism with a large apex angle (left).
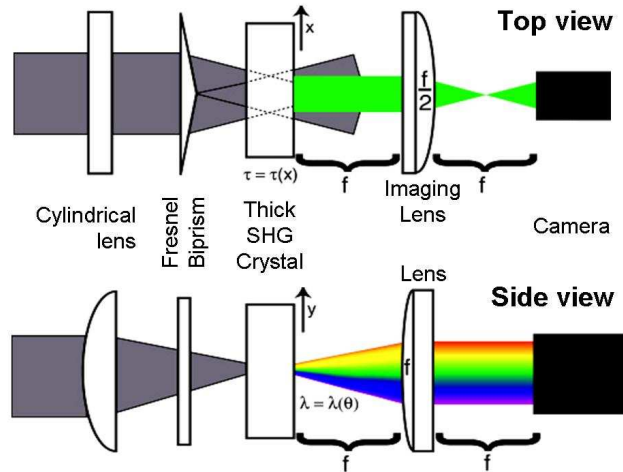

Fig. 3. Top and side views of GRENOUILLE. Use of the above anamorphic lens after the crystal yields a device with only four components.

The Fresnel biprism splits a 2cm beam into two 1cm-diameter beams, which, in order to attain a delay range of 20ps, requires a beam crossing angle of 30°. Unfortunately, a biprism in the geometries of Figs. 2 and 3 cannot accomplish this because total internal reflection occurs. Inverting the biprism so that it points toward the beam source might seem to solve this problem, but it yields beam overlap *inside the biprism*, not the SHG crystal.

To solve these problems, we modified the shape of the SHG crystal from the universally used rectangular shape to a *pentagonal* shape (see Fig. 4). This solves these problems and, even better, reduces the number of components in this already very simple device from four to as few as three (assuming a 2cm beam to begin with and an anamorphic lens after the crystal) [3], although in our first demonstration two lenses were used after the crystal, one for mapping wavelength to position and another for imaging the delay dimension.

Figure 4 shows a schematic of the GRENOUILLE design used in this experiment. Our beam was small, so we expanded it using a cylindrical telescope in the horizontal dimension and then focused it onto the crystal by a cylindrical lens in the vertical dimension.

The pentagonal crystal splits the pulse into two separate beams and crosses them as shown in Fig. 5(b), mapping delay onto horizontal position at the crystal and camera. The thick crystal phase-matches different colors for different angles in the other plane, which yields very small phase-matching bandwidths for the SHG beam. A vertical cylindrical lens then maps angle out of the crystal to vertical position at the camera, thus spectrally resolving the SHG beam in the vertical direction. The result is a single-shot SHG FROG trace at the camera with delay varying in the x-direction and wavelength varying in the y-direction. Of course, many pulses can be averaged if desired.
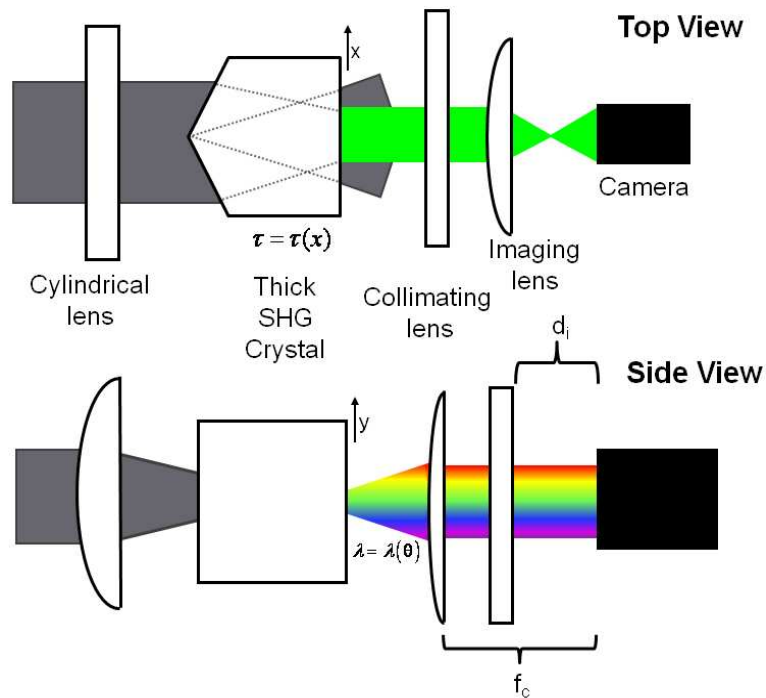

Fig. 4. The set-up for the ps GRENOUILLE. The schematic shows both the top view and the side view. The pentagon-shaped crystal both crosses the beams (top view) and angularly disperses the signal beam (side view). The collimating lens located a focal length, f_c, from the camera maps the angularly dispersed beam to position on the camera. The imaging lens is chosen to provide the depth of field necessary to image the entire width of the crystal. It is placed a distance d_i from the camera satisfying the imaging condition.

3. GRENOUILLE design

3.1 Crystal type and thickness

The first step in designing a GRENOUILLE for relatively long pulses is to determine the crystal type and thickness to yield sufficient dispersion to spectrally resolve the pulse. The use of a thick dispersive SHG crystal with high group velocity mismatch [GVM = $1/v_g(\omega)$ − $1/v_g(2\omega)$] results in a small phase matching bandwidth. This fact is embodied in the first important relation in GRENOUILLE theory:

$$GVM \cdot L >> \tau_p. \tag{1}$$

This relation places a lower limit on the spectral resolution of GRENOUILLE, where L is the crystal thickness and τ_p is the pulse width. Our device pushes Eq. (1) as far as possible, as described in [24]. In the experiments conducted in this paper a 4cm $LiIO_3$ crystal resulted in an upper limit of 23ps or the temporal range.

We cannot, however, increase GRENOUILLE's spectral resolution without limit by further increasing the thickness of the crystal. If the crystal is too thick, the input pulse will spread too much in time (distort) due to group velocity dispersion (GVD). This leads to the second important relation in GRENOUILLE theory:

$$GVD \cdot L << \tau_c, \tag{2}$$

where τ_c is the coherence length of the pulse, that is, its shortest temporal feature. Equation (2) puts a lower limit on the temporal resolution of GRENOUILLE. In the experiments conducted in this paper, a 4cm $LiIO_3$ crystal resulted in a lower limit of 200fs on the temporal resolution. This yields a device finesse (the ratio of the temporal range and resolution) of 115, an excellent value for the measurement of even complex, shaped pulses.

3.2 Apex angle and width of crystal

The second step in designing our ps GRENOUILLE is to match the dispersion introduced by the crystal to both the apex angle and width of the pentagon-shaped crystal.

In the original GRENOUILLE design [3], the Fresnel biprism separates the initial beam into two identical beams and crosses them inside the crystal. Here we do so using a pentagonal SHG crystal.
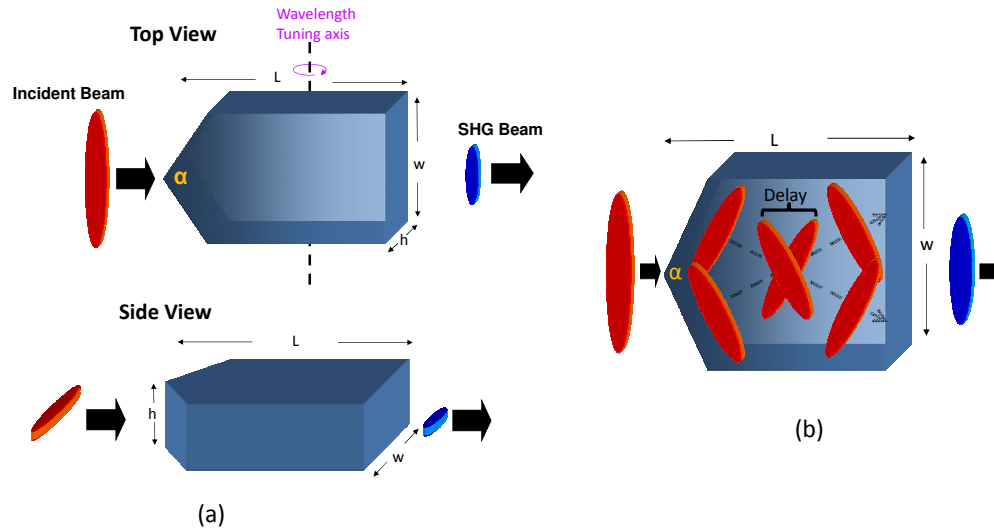
Fig. 5. a. The top and side views of the pentagonal SHG crystal. The top view also displays the axis about which the crystal can be rotated to tune the wavelength. b. The crossing of the signal beams inside of the crystal. This figure shows that by increasing the width of the beam, w, or the apex angle of the pentagon, α, the delay range is increased.

The pentagon shape forces the beams to begin crossing inside the crystal for all crossing/apex angles, thereby permitting a larger temporal range (see Fig. 5(b)). Increasing the beam width, w, increases the spatial extent of the two beams inside the crystal and so also increases the temporal range of the device.

3.3 Matching the dispersion (crystal thickness) and the temporal range (apex angle and width)

Any temporal or spectral measurement device requires sufficient temporal and spectral range and resolution. By the fundamental nature of the Fourier transform, the spectral (and temporal) resolution required to resolve a pulse is the reciprocal of its pulse length (or spectral width) and vice versa. Thus, in a well-designed GRENOUILLE, the spectral resolution (phase-matching bandwidth) achieved by the crystal *and* the delay range should be related by the uncertainty relation. If this is not the case, the GRENOUILLE trace will be distorted. Either delay information at large delays will be lost while fine spectral features resolved, or the opposite instance, fine spectral features will be unresolved while information at large delays is recorded on the trace. Both situations will impede the performance of the FROG algorithm. Therefore the three parameters; length, width, and apex angle of the pentagon are related. The approximate spectral resolution of the crystal is given by the full-width-half-maximum of the phase-matching bandwidth [24]:

$$\partial \lambda_{fwhm} = \frac{.44\lambda_0 / L}{\left| n'(\lambda_0) - \frac{1}{2} n'(\lambda_0 / 2) \right|}. \tag{3}$$

Because it provided the largest GVM for 800 nm, we chose a LiIO$_3$ crystal (cut at 60°). Additionally, we chose a very long thickness of 4cm. This provided $\delta\lambda_{fwhm} = 0.04$nm, which is sufficient spectral resolution to resolve any spectral structure in a pulse with a pulse length of 23ps.

The temporal range, 23ps, determined by the spectral resolution, should also match the temporal range achieved by the crossing beams. Figure 6 illustrates the ray tracing analysis of the beams inside the crystal.
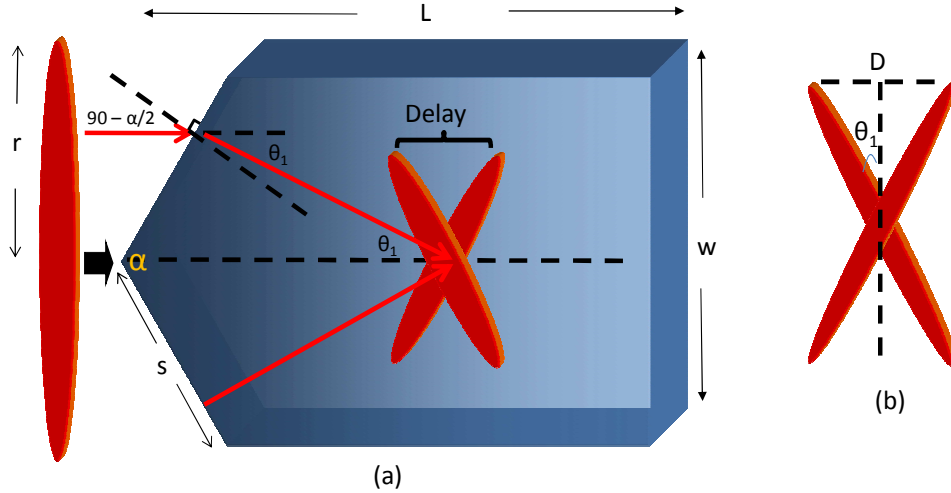
Fig. 6. a. The ray tracing diagram used to calculate the crossing angle of the two beams inside the crystal. b. The diagram used to calculate the range of delay inside the crystal.

The delay range of the GRENOUILLE depends on three parameters of the crystal, its apex angle, α; the index of refraction, n; and the width, w. First calculating the crossing angle, θ_1, we find using Fig. 6(a):

$$\theta_1 = 90 - \frac{\alpha}{2} - \sin^{-1}\left(\frac{1}{n}\cos\left(\frac{\alpha}{2}\right)\right). \tag{4}$$

Next, the maximum distance between the two edges of the crossing beams, D, shown in Fig. 6(b) is

$$D = s \sin\theta_1, \tag{5}$$

where s is the length of one of the beams inside of the crystal shown in Fig, 6(a), which, if the incident beam illuminates the entire width of the crystal, is

$$s = \frac{r}{\sin(\alpha/2)}. \tag{6}$$

The delay range is related to the maximum distance by

$$\Delta\tau = \frac{Dn}{c}, \tag{7}$$

where c is the speed of light in vacuum and n is the refractive index of the material.

Equation (4-7) yield the expression for the delay range of the crystal,

$$\Delta\tau = \frac{r}{c}\cot\frac{\alpha}{2}\left(\sqrt{n^2 - \cos^2\left(\frac{\alpha}{2}\right)} - \sin\left(\frac{\alpha}{2}\right)\right). \tag{8}$$

In our experiment a 2.7cm wide type-I LiIO$_3$ crystal with an apex angle of 126° yielded a temporal range of $\Delta\tau_{range}$ = 19.5 ps.

A smaller apex angle, α, yields a larger crossing angle and hence a larger delay range, which appears to come at a cost of adding more potentially beam-distorting angular dispersion to the pulse. Fortunately, we find that the angular dispersion is negligible. But a smaller apex angle also yields a shorter beam overlap length, potentially smaller than the full crystal thickness, which would increase the phase-matching bandwidth. In addition, GRENOUILLE

involves non-collinear SHG, and therefore is governed by the non-collinear SHG phase-matching condition:

$$n_e(2\omega) = n_o(\omega)\cos(\theta_1), \qquad (9)$$

where θ_1 is the crossing angle of the two beams inside the crystal (Fig. 6). Due to the cosine, phase matching unfortunately can cease to be possible at large crossing angles, or in the case of GRENOUILLE, small crystal apex angles.

Although Eq. (9) shows that, by reducing the apex angle of the crystal, the index of refraction of the material can be changed, thereby modifying the value of the phase-matching bandwidth given by Eq. (3), the dependence on the phase matching bandwidth and the crossing angle is negligible. Therefore, further reducing the apex angle of the crystal is *not* an effective way to increase the spectral resolution of GRENOUILLE unless the beam can be made larger and the noncollinear phase-matching condition can continue to be satisfied.

One characteristic of all GRENOUILLE designs is the effect of the spatial profile of the beam on the measured GRENOUILLE trace. This effect is simply a spatial intensity mask [25] and can be calculated from the measured spatial intensity profile of the beam. For longer pulses the spatial mask could reduce the intensity of features at large delays due to the beam intensity falling off at the crystal edges, which correspond to large delays. Such distortions can be removed by dividing the measured GRENOUILLE trace by the intensity mask. But, as has been shown previously, because GRENOUILLE uses such thick crystals, the beams cross through each other throughout the crystal, thus smearing out any distortions due to this effect, which is especially so for the current device, rendering this effect nearly irrelevant for this device, except for cases involving pulses as long as the time limit of the device that happen to have beam sizes that are too small [25].

Alternative crystal materials with high GVM values are listed below in Table 1 for other wavelength ranges at room temperature operation.

Table 1. Different possible crystal materials for varying wavelength ranges[a]

Material	Wavelength Range (nm)	Average GVM (fs/cm)
$LiIO_3$	700-900	6923
$LiNbO_3$	900-1200	7162
Ag_3AsS_3 (Proustite)	1200-2500	6733

[a]The average GVM corresponds to the average GVM over the wavelength range [26].

3.4 Depth of field

Another important aspect to consider when deciding upon the construction of a GRENOUILLE for measuring long pulses is the depth of field of the imaging system. In GRENOUILLE the depth of field of the imaging system must be approximately equal to or exceed the crystal thickness. If this condition is not met, fine trace structure will be out of focus and wash out [3].

Depth of field was not an issue in previous implementations of GRENOUILLE, which used crystals of thicknesses <5mm, because the depth of field requirement was met easily. However, as the thickness of the crystal increases, the depth-of-field requirement becomes more difficult to satisfy.

To check this condition for our device, assume that the crystal center is a distance d_o away from the lens and is perfectly imaged onto a camera a distance d_i from the lens. Next, we consider a potentially out-of-focus front surface at a distance $\varepsilon + d_o$ from the lens, which will be acceptably in focus if

$$\varepsilon = 2d_o r_c / Md, \qquad (10)$$

where r_c is the required spatial resolution at the camera, M is the magnification of the imaging system, and d is the diameter of the beam on the lens. In our experiment, using an imaging

lens with a focal length of 150mm to image the crystal at an object distance of 600mm yielded a depth of field of 6.4cm. We experimentally determined the required spatial resolution to be roughly 50pixels or 0.175mm after performing a similar GRENOUILLE experiment and noting the delays at which the trace began to wash out.

3.5 Minimum pulse energy required for GRENOUILLE

An important parameter to consider is the pulse energy required for the modified GRENOUILLE to work.

The detector arrays for all GRENOUILLEs are cameras that are composed of pixels that register a number of counts proportional to the number of incident photons. Roughly 700 blue (400nm) photons are required to register a count of 100 on a 10-bit pixel in a CMOS camera array. Additionally, a FROG trace for a complex pulse may require a 128 × 128 array size. Therefore, a minimum of $700 \times 128^2 \sim 11$ million photons would be required to generate the trace, and the minimum energy required to generate the FROG trace would be

$$E_{min} = N \frac{hc}{\lambda} = 5.7 \text{pJ} \qquad (11)$$

where N is the number of photons. If the signal is time averaged over the frame rate (~30fps for standard CMOS cameras), a minimum average power, $P_{min} = 190 \text{pW}$, is necessary to measure a complex pulse.

Next, this minimum power must be related to the power of the SHG signal beam, P_{SHG}, generated by the crystal. But before we can do that, P_{SHG}, must be written in terms of the parameters of the GRENOUILLE and laser source. The power of the SHG signal beam is

$$P_{SHG} = I_{SHG} w_x w_y \tau_p r, \qquad (12)$$

where I_{SHG} is the intensity of the SHG beam, w_x is width of the crossing beams inside the crystal in the delay dimension (the value s in Fig. 6(a)), w_y is the focused size of the beam (Fig. 4, side view), τ_p is the pulse length, and r is the repetition rate of the laser. The intensity of the SHG beam is given by [4] as

$$I_{SHG} = \frac{8\pi^2 \eta_0 d^2 I_{in}^2 L^2}{\lambda^2 n^3}, \qquad (13)$$

where $\eta_0 = c\mu_0$, c is the speed of light in vacuum, d is the d-coefficient of the crystal defined as $d = \chi^{(2)}/2$, L is the length of the crystal, λ is the fundamental wavelength, n is the index of refraction of the crystal, and I_{in} is the intensity of the input beam

$$I_{in} = \frac{E_{in}}{w_x w_y \tau_p}, \qquad (14)$$

where E_{in} is the energy of the input pulse. Additionally, the length of the crystal, L, should be matched to the confocal parameter of the focused beam [3] resulting in the relation

$$L = \frac{2\pi w_y^2}{\lambda}. \qquad (15)$$

Equation (12-15) can be used to solve for the power of the signal beam

$$P_{SHG} = \frac{8\pi^2 \eta_0 d^2 E_{in}^2 L^{3/2} \sqrt{2\pi}}{w_x \lambda^{5/2} n^3 \tau_p} r. \qquad (16)$$

Now that P_{SHG} is written in terms of the GRENOUILLE and laser source parameters, the minimum energy for GRENOUILLE can be determined. Using the minimum average power

required for a FROG trace as P_{SHG} in Eq. (16), and solving for E_{in} yields the minimum energy required for GRENOUILLE to work

$$E_{min} = \sqrt{\frac{\lambda^{5/2} n^3 w_x \tau_p P_{min}}{8\pi^2 \eta_0 d^2 L^{3/2} r \sqrt{2\pi}}}. \qquad (17)$$

In the experiments performed in this paper, L = 4cm, n ~1.9, λ = 800nm, τ_p ~10ps, d ~4.4pm/V [26], w_x ~1.2cm, and r = 76MHz which yields a minimum energy of E_{min} ~.3pJ per pulse, or multiplying E_{min} by the repetition rate, r, determines the minimum average power, P ~25μW.

Note that, in a GRENOUILLE, the length of the crystal is determined by the spectral resolution required to measure the pulse. If we write the spectral resolution required to resolve the pulse as $\delta\omega \approx 0.5/(TBP~\tau_p)$, and use Eq. (3), we see that the crystal length must be proportional to the pulse length. Substituting this result into Eq. (17), we find that the minimal average power measurable by a properly designed GRENOUILLE scales *inversely* with the fourth root of the pulse length. Although this is a weak dependence, it is somewhat unintuitively the case that, due to the various partially cancelling factors, the longer the pulse the more sensitive the GRENOUILLE—provided that a device can be designed.

4. Experiment

We performed measurements using a Coherent MIRA Ti:Sapphire oscillator and a Coherent Legend-F regenerative amplifier. The first experiment involved a 5ps double pulse from the MIRA, which emitted pulses centered at 802nm with a FWHM bandwidth of 2.5nm, a repetition rate of 76MHz, and pulse energy of 5.2nJ per pulse. The second experiment involved the measurement of a train of pulses. To generate the train of pulses, higher pulse energies were required. For this experiment, we used pulses from the Legend-F regenerative amplifier, centered around 800nm and filtered with a 3nm-wide bandpass filter. The Legend-F amplifier system emitted pulses at a repetition rate of 1kHz and pulse energies of 3mJ per pulse.

In all our experiments, the incident beam had an initial beam diameter of ~2mm, and it was magnified by a factor of 20 in the delay dimension in order to ensure uniform beam intensity over the entire face of the crystal. Then the beam was focused onto the pentagonal LiIO$_3$ crystal using a 100mm focal length cylindrical lens.

The crossing beams in the crystal were then imaged onto the camera by a single 150mm focal-length cylindrical lens. Additionally, a 400mm focal length cylindrical lens oriented perpendicular to the imaging lens mapped the crystal exit angle to position at the camera. For experimental simplicity, these two lenses are usually combined into one anamorphic lens, but we have used two here for flexibility in these proof-of-principle measurements. In the second experiment, using the Legend-F regenerative amplifier, a 300mm focal length lens was used to fit the entire 3nm bandwidth of the incident beam on the camera. Lastly, a blue low-pass filter removed the 800nm light from the SHG beam. A CMOS camera located 800mm away from the crystal collected the image.

5. Results and discussion

We performed two experiments to demonstrate our ps GRENOUILLE's capabilities. These measurements highlighted, not only its ability to measure the intensity and phase of complex ps pulses, but also its high spectral resolution relative even to a conventional high-resolution spectrometer.

In the first experiment using the MIRA laser, we measured a 5.5ps double pulse. The double pulse was created using a Michelson interferometer. Figure 7 shows the measurement of a 5.5ps (separation) double pulse.
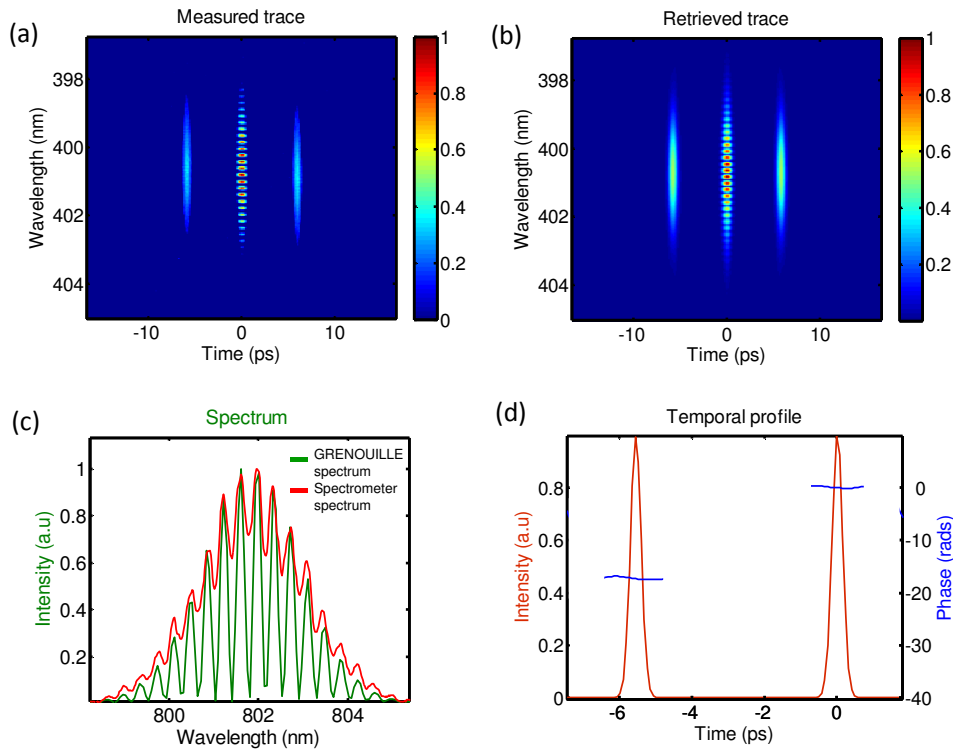
Fig. 7. a. The measured ps GRENOUILLE trace for a 5.5ps double pulse. b. The retrieved GRENOUILLE trace. c. The GRENOUILLE retrieved spectrum compared with that of a high resolution spectrometer with 0.01nm spectral resolution. The high contrast fringes demonstrate the high resolution of GRENOUILLE compared to a conventional spectrometer. d. The retrieved temporal intensity and phase of the 5.5ps pulse. As expected, the retrieved temporal intensities of the pulses were equal.

To verify the accuracy of our measurement, we compared the GRENOUILLE-measured spectrum to that measured by a commercial high-resolution spectrometer with 0.01nm spectral resolution (Ocean Optics HR4000 spectrometer). The pulse's high-contrast fringes demonstrate GRENOUILLE's high spectral resolution compared to that of the commercial spectrometer. This high contrast—significantly better than our calculated value!—is a result of a combination of effects, including the thick crystal, the ability of the FROG algorithm to see otherwise washed out structure, and our deconvolution of the spectral response function from the results using a Lucy-Richardson deconvolution algorithm (a standard procedure in the GRENOUILE pulse-retrieval code [27]). This deconvolution algorithm functions to improve the spectral resolution without introducing any complexity to the device and is a commonly used procedure in image processing and spectral measurements [28], and it is standard in commercial GRENOUILLE software.

Next, we measured a train of pulses, made by passing the beam from the Coherent Legend-F through an etalon composed of two 90% partially reflecting mirrors. This measurement highlighted GRENOUILLE's ability to measure more complicated temporal and spectral profiles. Figure 8(c) shows the agreement between the GRENOUILLE-retrieved spectrum and the spectrum measured by the spectrometer.
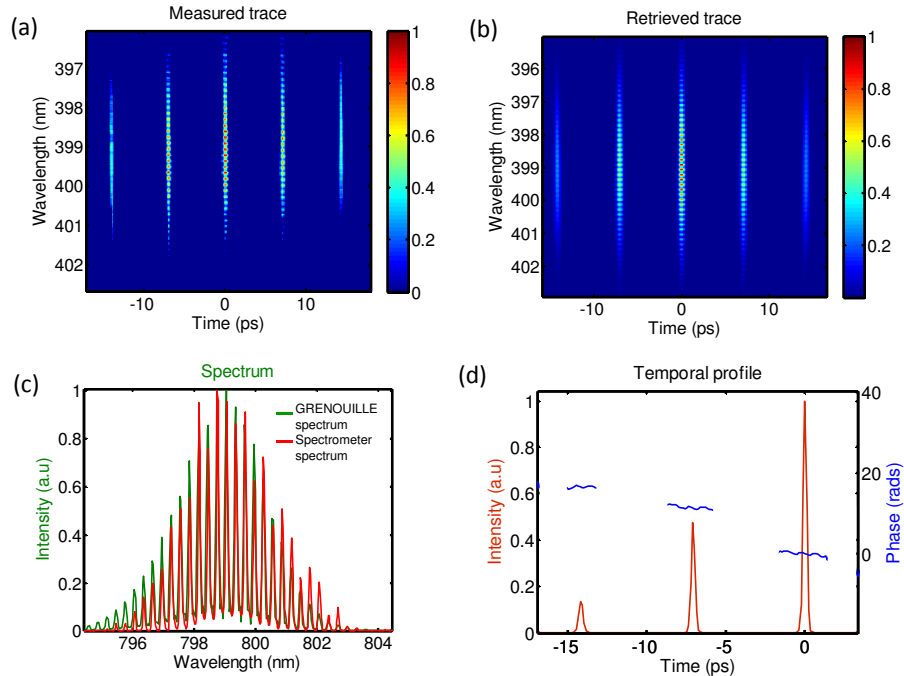
Fig. 8. a. The measured GRENOUILLE trace for a train of pulses. b. The retrieved GRENOUILLE trace. c. The GRENOUILLE retrieved spectrum compared with that of a spectrometer. The agreement between the two independent measurements confirms GRENOUILLE's capabilities. d. The retrieved temporal intensity and phase of the train of pulses.

Figure 8(d) shows the retrieved temporal profile of the ~15ps train of pulses. As expected, the intensities of the pulses in the pulse train decreases with time because the pulse train was generated with an etalon composed of two 90% partially reflecting mirrors.

Although the temporal profile of the measurement in Fig. 8(d) is relatively simple, the spectral profile is complex, and GRENOUILLE should be capable of measuring pulses with even more complex temporal profiles, because the FROG algorithm has proven capable of measuring pulses with time-bandwidth products greater than 1000 [16]. Our device, with its finesse of over 100, should be capable of measuring pulses with complexities (time-bandwidth products) up to almost this value.

To extend GRENOUILLE to even longer-pulse measurement would involve increasing the delay range by reducing the apex angle of the pentagon. While this yields a potentially shorter beam overlap region, a larger beam and corresponding larger width of the crystal could compensate for this effect. Use of a more dispersive crystal would also help; however, most applications for nonlinear crystals generally prefer less dispersive crystals, so such crystals may be difficult to obtain. As a result, a clever new idea would be preferable to achieve the measurement of even longer pulse lengths in a simple manner.

6. Conclusion

We have extended the GRENOUILLE technique for simple ultrashort-laser-pulse measurement to pulses up to ~15ps in length by replacing the Fresnel biprism and rectangular SHG crystal in the standard GRENOUILLE design with a single pentagonal SHG crystal. This reduces the number of components to as few as three (two lenses and the pentagonal crystal), making for an extremely simple, alignment-free device, whose convenience in pulse measurement seems unparalleled.

Acknowledgement